Increased stability of mercapto alkane functionalized Au nanoparticles towards DNA sensing

2010 Nanotechnology 21 285608

(http://iopscience.iop.org/0957-4484/21/28/285608)

Nanotechnology **21** (2010) 285608 (8pp) doi:10.1088/0957-4484/21/28/285608

Increased stability of mercapto alkane functionalized Au nanoparticles towards DNA sensing

H Jans[1,2], T Stakenborg[1], K Jans[1], B Van de Broek[1,2], S Peeters[1,3], K Bonroy[1,4], L Lagae[1], G Borghs[1] and G Maes[2]

[1] IMEC, Functional Nanosystems, Kapeldreef 75, B-3001 Leuven, Belgium
[2] KULeuven, Physical and Quantum Chemistry, Celestijnenlaan 200F, B-3001 Leuven, Belgium
[3] KULeuven, Medical Diagnostic Science, Minderbroedersstraat 10 B-3000, Leuven, Belgium

E-mail: Hilde.Jans@imec.be

Received 4 May 2010
Published 28 June 2010
Online at stacks.iop.org/Nano/21/285608

Abstract

The use of gold nanoparticles (GNPs) in bioassays is often hampered by their colloidal stability. In this study, gold nanoparticles coated with different mercapto alkanes were investigated towards their stability. Hereto, the effects of the alkane chain length (5–11 methylene groups), the type of functional end-group (–OH or –COOH) and the amount of incorporated poly-ethylene oxide units (none, 3 or 6) on the GNP stabilization was evaluated. Based on these results, an optimal mercapto alkane ($HS(CH_2)_{11}PEO_6COOH$) was selected to increase the colloidal stability up to 2 M NaCl. Furthermore, it was proved that this mercapto alkane is ideally suited to enhance the stability of DNA functionalized GNPs in high electrolytic hybridization buffers. The effectiveness of these DNA functionalized GNPs was demonstrated in a sandwich assay using a surface plasmon resonance biosensor. The superior stability of these nanoparticles during hybridization may lead to enhanced biosensor technologies.

1. Introduction

Noble metal nanoparticles are interesting study objects due to their unique size-dependent physical properties. In particular, the localized surface plasmon resonance (LSPR) of gold nanoparticles (GNPs) is a well-known phenomenon associated with the collective oscillation of conduction electrons on the surface upon interaction with an electromagnetic field [1–3]. The wavelength position of the plasmon band does not only rely on the size and shape of the metal nanoparticles [4], but more importantly, depends on the refractive index of the surrounding medium and hence, on the attached molecules [5]. These LSPR properties of GNPs have been used in several areas, for instance biosensing [6–9] and molecular imaging [10] for which it is of utmost importance that the particles retain their stability and targeting properties during the different manipulation steps. Especially when nanoparticles are used in more complex clinical samples (e.g. serum) or high salt buffers (e.g. during hybridization), aggregation remains of major concern [11, 12].

The most straightforward way to modify the GNP surface is the use of mercapto alkanes [13]. These latter molecules are particularly known to form self-assembled monolayers (SAMs) onto 2D gold surfaces by means of chemisorption. The van der Waals interactions between neighboring, sufficiently long alkane chains as well as intermolecular hydrogen bonds and the possible occurrence of cross-linker groups within the alkane chain can lead to the formation of rigid SAM structures [14]. Additional groups, mainly poly(ethylene oxide) units (PEO), can be incorporated into the mercapto alkanes to make them more hydrophilic and resistant to non-specific interactions with matrix proteins [15, 16]. To modify GNPs with mercapto alkanes [17] several approaches have been reported such as a one-pot synthesis [18], a two-step approach [19], as well as place-exchange reactions [20–22].

For use in possible biomedical applications, these chemically functionalized GNPs can be further modified with

[4] Present address: Tibotec-Virco, Generaal De Wittelaan 11, B-2800, Mechelen, Belgium.

Table 1. Characteristics of GNPs coated with different mercapto alkanes.

Coating[a]		Hydrodynamic diameter (nm)[b]	$\Delta\lambda_{LSPR}$ (nm)[c]	Zeta potential (mV) (pH = 8)[d]	NaCl (M)[e]
Citrate	—	18.5 ± 0.2	—	-42.5 ± 1.3	0.03
HS–$(CH_2)_5$–COOH	**(1)**	>5 μm	± 180	—	—
HS–$(CH_2)_6$–OH	**(2)**	>5 μm	± 105	—	—
HS–$(CH_2)_{11}$–OH	**(3)**	779.0 ± 104	± 58	—	—
HS–$(CH_2)_{10}$–COOH	**(4)**	21.5 ± 0.8	4.1 ± 0.5	-48.6 ± 1.6	0.12
HS–$(CH_2)_6$–PEO_3–OH	**(5)**	19.6 ± 0.4	5.0 ± 0.3	-22.3 ± 0.9	0.50
HS–$(CH_2)_6$–PEO_3–COOH	**(6)**	21.6 ± 1.2	2.3 ± 0.5	-49.4 ± 0.5	1.00
HS–$(CH_2)_{11}$–PEO_3–OH	**(7)**	19.1 ± 0.5	5.5 ± 0.4	-15.5 ± 0.5	0.50
HS–$(CH_2)_{11}$–PEO_6–COOH	**(8)**	25.6 ± 0.9	3.9 ± 0.5	-70.0 ± 8.0	2.00

[a] The various mercapto alkanes are numbered from 1 to 8.
[b] The hydrodynamic diameter of the various GNPs after synthesis is measured by DLS.
[c] The wavelength shift ($\Delta\lambda_{LSPR}$ (nm)) due to the exchange reaction, where citrate is replaced by mercapto alkanes, is presented.
[d] Additionally, the zeta potential of the GNPs coated with different capping agents is reported.
[e] The values represent the maximum concentration NaCl at which the GNPs do not show aggregation and hence also no λ_{LSPR} shift.

specific end-groups which allow further covalent attachment of biomolecules [23]. Despite several efforts to improve the stability and targeting properties of these biofunctionalized nanoparticles, their performance is still not ideal. Traditional synthesis routes such as the covalent attachment of DNA onto pre-activated GNPs and the conventional biotin–avidin binding chemistry are commonly used, in spite of their low yields [24]. The simultaneous chemisorption of thiolated DNA in combination with stabilizing mercapto alkanes is therefore an excellent option to achieve DNA loaded GNPs with enhanced stability [25, 26].

In this work, place-exchange reactions were investigated to remove loosely bound citrate molecules of traditionally synthesized GNPs by mercapto alkanes. The effect on the stability by changing the alkane chain length, the amount of PEO-units present in the chain and the influence of charged carboxylic end-groups compared to hydroxylic ones were investigated in detail. Furthermore, we evaluated the simultaneous chemisorption of mercapto alkanes and thiolated DNA to obtain highly stable DNA functionalized GNPs. These GNPs were fully characterized by both, UV–vis absorption spectroscopy and dynamic light scattering. Furthermore, the specific recognition of complementary ssDNA in high salt hybridization buffer was proven using surface plasmon resonance as a characterization technique.

2. Experimental details

2.1. Materials

All mercapto alkanes used are numbered for clarity as shown in table 1. 1-mercapto-11-undecyl-tri(ethylene glycol) ($SH(CH_2)_{11}PEO_3OH$) (**7**) and the corresponding carboxylic derivative ($SH(CH_2)_{11}PEO_6COOH$) (**8**) were obtained from SensoPath Technologies (Montana, USA). Trisodium citrate was purchased from Acros (Geel, Belgium) and 1-mercapto-hexanol ($SH(CH_2)_6OH$) (**2**) from Fluka (Buchs, Switzerland). 1-mercapto-6-hexyl-tri(ethylene glycol) ($SH(CH_2)_6PEO_3OH$) (**5**) was synthesized in house [16], whereas its carboxylic derivative ($SH(CH_2)_6PEO_3COOH$) (**6**) was purchased from Prochimia (Sopot, Poland). All other chemicals, including tetra-chloroauric acid ($HAuCl_4$) and 6-mercaptohexanoic acid ($SH(CH_2)_5COOH$) (**1**), 11-mercaptoundecanol $SH(CH_2)_{11}OH$ (**3**) and 11-mercaptoundecanoic acid ($SH(CH_2)_{10}COOH$) (**4**) were obtained from Sigma-Aldrich (Missouri, USA). The oligonucleotide used, a probe of 25 nucleotides (5′TTCACAGGTACTGGATTTGATT GTG) (25-nct), was synthesized and modified with a 5′-mercapto-11-undecyl hexa(ethylene oxide) linker (25-nct-11) by Van Aerschot [27]. The same oligonucleotide and its complementary probe (5′CACAATCAAATCCAGTACCTGT GAA) (25-nct-c) were modified both with a 5′-mercapto-hexanol linker (25-nct-6, 25-nct-c-6) and derived from Eurogentec (Seraing, Belgium). Furthermore, an oligonucleotide (5′ACAGTCATTCCTGTCAACTGAGCAC) modified with a 3′-mercapto propanol linker (25-nct-3) was obtained from IBA GmbH (Göttingen, Germany). The complementary probe of 50 nucleotides (5′GTGCTCAGTTGACAGGAATGACTGTCAC AATCAAATCCAGTACCTGTGAA) (50-nct) was obtained from Eurogentec (Seraing, Belgium). All materials and reagents were used as received.

2.2. Synthesis of citrate stabilized GNPs

GNPs were prepared according to the method of Turkevich *et al* [28, 29]. Prior to the synthesis, all glassware was cleaned with a mixture of HCl/HNO_3 (3:1) and thoroughly rinsed with water. Briefly, 100 ml of an aqueous chloroauric acid solution (0.01% (w/v)) was boiled after which 3.6 ml of a filtered sodium citrate solution (1% (w/v)) was quickly added. When the GNPs were formed, indicated by a stable red color, the solution was boiled for an additional 10 min and left to cool down to room temperature. The GNPs were stored at 4 °C.

2.3. Synthesis of mercapto alkane functionalized GNPs

The citrate stabilized GNPs were modified with mercapto alkanes as described by Lin *et al* [18]. To maintain the colloidal

stability during reaction, the basicity of the citrate stabilized GNPs was adjusted to pH 11 by addition of NaOH (0.5 M). Subsequently, 200 μl of the mercapto alkanes (10 mM in ethanol) listed in table 1 were added to 2 ml of GNPs. The total suspension was stirred for 3 h. To remove the excess of free mercapto alkanes, the GNPs were centrifuged at a speed of 7500 rpm (rotor radius 99.83 mm) for 30 min. Finally, the pellet of GNPs was resuspended in 2 ml of water after decantation of the supernatant.

2.4. Synthesis of GNPs functionalized with a mixture of mercapto alkanes and DNA

One hundred microliters of a mercapto alkane solution (50, 100, 200 μM in ethanol) was added to 2 ml of GNPs previously adjusted to pH 11 (resulting in final concentrations of 2.3, 4.5 and 9.0 μM). After stirring the mixture for circa 10 min, 25-nct-11 (100 μl, 20 μM) dissolved in hybridization buffer (1.0 M NaCl, 10 mM Tris-HCl and 2 mM ethylenediaminetetraacetic acid (EDTA), pH 7) was added and incubated overnight. To remove the excess of free mercapto alkanes and 25-nct-11, the GNPs were centrifuged and resuspended in a 2 ml hybridization buffer.

2.5. Study of the LSPR properties of mercapto alkane functionalized GNPs

The wavelength at maximal absorbance (λ_{LSPR}) of the GNPs was determined from the UV–vis absorption spectrum measured with a data interval of 0.1 nm (Shimadzu UV-2550, Kyoto, Japan) before and after the chemisorption of mercapto alkanes. Deionized water was used as a blank sample for background subtraction. The λ_{LSPR} will show a small shift when the various mercapto alkenes are successfully chemisorbed onto the GNP surface and a large shift when the GNPs aggregate [30]. At least two independent experiments were performed using freshly prepared GNPs. Furthermore, within each experiment the measurement was repeated to determine the reproducibility.

2.6. Study of the GNP characteristics: size, polydispersity and zeta potential

The GNP size, polydispersity and zeta potential were investigated using dynamic light scattering (DLS) (Malvern Zetasizer Nano ZS, Worcestershire, United Kingdom). All sizes reported are volume averages based on three measurements. In addition, the nanoparticles size and monodispersity was determined using transmission electron microscopy (TEM) (FEI Tecnai F30, Oregon, USA) operating at 300 kV. The position and width of the measured plasmon band is related to the size and polydispersity of the GNPs respectively [31, 32].

2.7. Salt induced stability study of the various GNPs

To determine the lowest amount of mercapto alkanes necessary to stabilize the GNPs, their concentration in the synthesis protocol was varied (0.001, 0.01, 0.1, 1 and 10 mM) and the λ_{LSPR} was determined by UV–vis spectroscopy, measured with a data interval of 0.1 nm. The NaCl induced aggregation (hence stability) was studied by mixing equal volumes of the GNPs and NaCl together prior to the UV–vis absorption measurement. A data interval of 0.5 nm was used to observe the change in LSPR during the stability tests. The final concentration of NaCl, causing no change in the absorption spectrum (λ_{LSPR}), was reported. All stability studies were repeated at least two times using freshly prepared GNPs.

2.8. DNA binding studies using surface plasmon resonance

The surface plasmon resonance technique (SPR) (GE Healthcare Biacore 2000®, Cardiff, United Kingdom) was used to prove the potential of DNA modified GNPs. First, the hybridization efficiency of DNA modified GNPs was determined. The operation temperature was set at 20 °C and a flow rate of 5 μl min^{-1} was chosen during all measurements. The probes were immobilized as described earlier [33, 34]. Briefly, the gold sensor chip was cleaned by rinsing the gold surface with acetone followed by incubation for 15 min in an UV/O_3 chamber equipped with an ozone producing mercury grid lamp (BHK Inc., Illinois, USA) to remove all organic contaminants. To determine the hybridization efficiency of the DNA modified GNPs, thiolated DNA probes (300 μl, 25-nct-6/25-nct-c-6; 10 μM), dissolved in immobilization buffer (1 M KH_2PO_4, pH 3.8), were injected over the cleaned gold sensor surface during 1 h. The 25-nct-c-6 served as a specific probe and was immobilized on three lanes on the gold sensor surface. A non-specific control, 25-nct-6, was immobilized on lane 4. After probe immobilization, $SH(CH_2)_6OH$ (150 μl, 1 mM in H_2O) was injected to form a dense mixed monolayer [34, 35]. After rinsing the surface, GNPs functionalized with complementary ssDNA (100 μl, 25-nct-11, 1.4×10^{10} nanoparticles ml^{-1}, hybridization buffer) were allowed to hybridize for 20 min. After rinsing, the hybridization efficiency (expressed in resonance units RU) was determined.

Second, the potential of DNA modified GNPs was evaluated towards the detection of 50-nct in a sandwich approach. Therefore, 25-nct-3 (300 μl, 1 μM in 1 M KH_2PO_4 (pH 3.8)) was immobilized on a clean gold surface on all four lanes. Additionally, $SH(CH_2)_6OH$ (100 μl, 1 mM in H_2O) was injected. The complementary probe (50-nct) was allowed to hybridize for 20 min (0–160 nM). Furthermore, GNPs functionalized with ssDNA (100 μl, 25-nct-11, 1.4×10^{10} nanoparticles ml^{-1} in hybridization buffer) were allowed to hybridize for 20 min. The sensor surface could be regenerated using 20 μl NaOH (10 mM). The signal for both the hybridization of 50-nct and the hybridization of DNA functionalized GNPs was determined. The reproducibility of both studies was evaluated by conducting two independent experiments.

3. Results and discussion

3.1. Characterization of the citrate stabilized GNPs

The synthesis method applied yielded monodisperse spherical GNPs of 16 ± 1.2 nm as presented in the TEM image

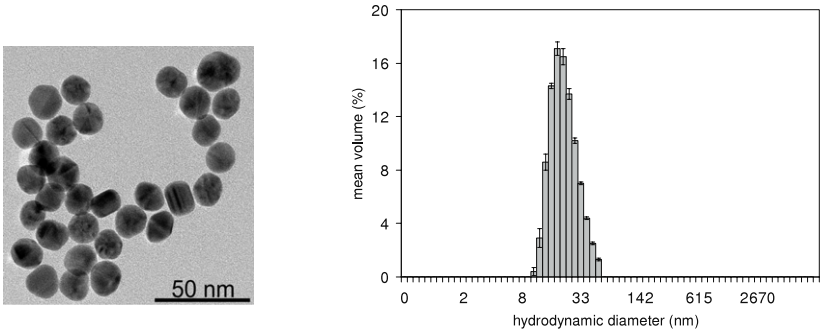

Figure 1. (a) TEM image of citrate coated GNPs. (b) The corresponding hydrodynamic diameter of citrate coated GNPs measured by DLS.

of figure 1(a). Similar observations were deduced from DLS measurements as the GNP showed a relatively small hydrodynamic size distribution centered at 18.5 ± 0.2 nm (figure 1(b)). Additionally, the UV–vis absorption spectra of the GNPs showed a very narrow plasmon bandwidth of 75 nm, centered at 518 nm, confirming the observations made by TEM and DLS. From all these observations, and assuming total reduction of the gold salt, the concentration of the citrate capped gold nanoparticles was calculated to be 1.4×10^{12} nanoparticles ml^{-1}, which is in agreement with previous reports [27, 36].

3.2. Characterization of GNPs coated with mercapto alkanes

The synthesized citrate stabilized GNPs were conjugated with a variety of mercapto alkanes (listed in table 1). The effect of the alkane chain length, the incorporation of PEO-units and the use of different end-groups on the hydrodynamic diameter, the LSPR characteristics and the zeta potential was investigated in detail.

The Brownian motion of the particles and hence the measured hydrodynamic diameter is very sensitive to 'soft' flexible molecules (e.g. polymers) as the latter can cause significant friction drag [37]. Therefore, it is natural to assume that DLS is an excellent technique to study the differences in the GNPs coatings [38] with mercapto alkanes. As shown in table 1 and in agreement with previous reports [30], the use of mercapto alkanes **1** and **2** during synthesis did not result in successfully coated GNPs as they aggregated irreversibly, which could also be observed by eye (>5 μm). An inefficient coating was also observed for mercapto alkane **3**, albeit with a lower level of aggregation (<1 μm). This small improvement originates from a better inter-chain interaction by increasing the chain length (from 6 to 11), leading to a more compact SAM coating. A successful GNP coating was obtained by using mercapto alkane **4** [30]. In the latter case, the hydrodynamic size only increased by 3 nm (21.5 nm) compared to the citrate stabilized GNPs (18.5 nm). As such, changing the end-group of mercapto alkanes (of identical chain length) from –OH (**3**) to –COOH (**4**) resulted in a successful coating. This can likely be explained by a greater hydration of the carboxylic end-groups compared to the hydroxyl end-groups, keeping the GNPs dispersed. All investigated mercapto alkanes, equipped with PEO-units (**5**–**8**), resulted in successfully coated GNPs. In the latter case, coating thicknesses of 0.6 up to 7.1 nm were observed. Increasing the alkane chain length from 6 to 11 had no effect on the hydrodynamic diameter of GNPs coated with PEO equipped mercapto alkanes (**5**, **7**). By increasing the amount of PEO-units from 3 to 6 the hydrodynamic diameter clearly increased by 4 nm (**6**, **8**). This can be explained by both the enlarged size and improved hydration, due to extra PEO-units.

The DLS data were verified by UV–vis absorption spectroscopy. The λ_{LSPR} changed dramatically for mercapto alkanes **1**–**3**, indicating aggregation, while a much smaller λ_{LSPR} shift (<6 nm) was observed for the successfully coated GNPs with mercapto alkanes **4**–**8**. The $\Delta\lambda_{LSPR}$ changed only slightly upon an increase in alkane chain length from 6 to 11 (**5**, **7**) in contrary to a larger change for increasing amounts of PEO-units (**6**, **8**). Malinsky *et al* clearly demonstrated that the plasmon wavelength of silver nanoparticles is red shifted proportional to the length of the mercapto alkanes used [39]. A similar conclusion was drawn for the amount of PEO-units influencing the LSPR properties of a GNP film [40]. These findings are in relation with our observations on GNPs.

Overall, the UV–vis data are in agreement with the DLS measurements, although some small differences between both techniques could be observed. A more pronounced λ_{LSPR} shift (>5 nm) is obtained for the coatings containing mercapto alkanes with a hydroxylic end-group (**5**, **7**) compared to the corresponding carboxylic ending mercapto alkane (<4 nm) (**6**, **8**). This observation is in contradiction to their hydrodynamic diameters, (respectively <1.1 and >3 nm). Although mercapto alkanes of various chain lengths and PEO-units (bearing the same functional end-group) are red shifting the LSPR, this could not be observed for the total mercapto alkane chain length. This discrepancy is probably a result of the difference in refractive index of the various mercapto alkanes, which is not in relation to the thickness of the mercapto alkane layer surrounding the GNPs. In this way, the latter results are not totally comparable to the DLS measurements.

To further characterize the mercapto alkane coatings of the GNPs, their zeta potential at pH 8 was measured as shown in table 1. Carboxylic terminated mercapto alkanes (**4**, **6**, **8**) gave a negative charge of <−45 mV, while hydroxylic ending mercapto alkanes (**5**, **7**) displayed a less negative zeta potential (>−25 mV). Carboxylic groups are charged

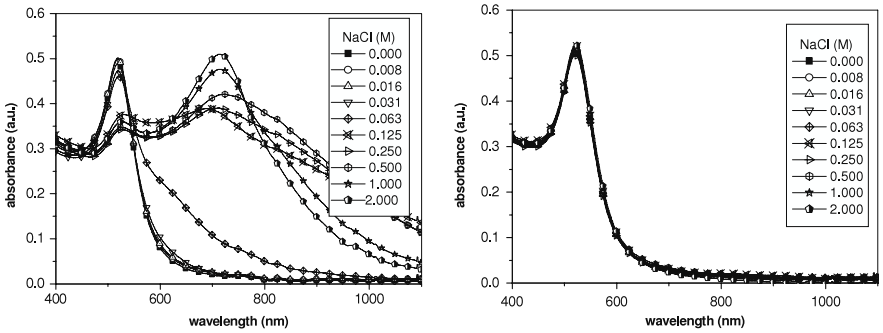

Figure 2. (a) Induced aggregation of citrate coated GNPs by NaCl measured with UV–vis absorption spectroscopy. (b) UV–vis absorption spectra of HS–$(CH_2)_{11}$–PEO_6–COOH coated GNPs with different concentrations of NaCl.

in water at pH's larger than their pI [41]. On the other hand, hydroxyl groups are easily hydrated but not easily ionized in solution. Although, deprotonation can occur at high pH values leading to a remaining negative charge on the GNPs [42]. Naturally, no accurate zeta potential could be measured for mercapto alkanes **1**–**3** because of their aggregated state. Remarkably, an extreme negative zeta potential was measured for mercapto alkane **8** (−70 mV) compared to the other carboxylic terminated mercapto alkanes (**4**, **6**). The different degree in hydrophilicity is reflected in the magnitude in zeta potential in the alkaline range where the adsorption of OH^- ions compensate for H_2O adsorption onto the mercapto alkane SAM [43]. This observation was previously confirmed by the large increased hydrodynamic diameter, and hence higher hydrophilicity of mercapto alkane **8** compared to the other stabilizing mercapto alkanes (**4**–**7**). As such, the zeta potential measurements proved the successful coating of GNPs with mercapto alkanes **4**-**8** and allowed to distinguish between carboxylic and hydroxylic terminated mercapto alkanes at a fixed pH.

In conclusion, DLS, UV–vis absorption spectroscopy and zeta potential measurements proved the successful coating of mercapto alkanes **4**–**8** onto the GNP surface. Furthermore, these techniques allow the observation of differences in the characteristics and quality of the various SAMs coating the GNPs.

3.3. Stability study of the GNPs coated with different mercapto alkanes

3.3.1. Citrate versus mercapto alkanes. For many biomedical applications, it is important that the GNPs are stable in highly electrolytic environments. To characterize this electrolytic stability of citrate stabilized GNPs, salt induced aggregation experiments were performed [44]. By increasing the concentration of NaCl to 0.03 M, the corresponding UV–vis absorbance spectra were indistinguishable, indicating that the nanoparticles preserve their stability (figure 2(a)). Upon further increase of the NaCl concentration the absorbance at 518 nm decreased and a second band in the UV–vis spectrum was observed around 700 nm, indicating nanoparticle aggregation. This additional band is a result of plasmon coupling and is in agreement with previous reports [27]. The observed aggregation can largely be explained by the DLVO theory (Derjaguin, Landau, Verwey, Overbeek [45]) which states that the stability of a colloidal suspension is determined by an electrostatic repulsive, Coulombic force, which drives particles apart and by attractive van der Waals forces which promote particle aggregation. The colloidal stability can easily be disrupted by addition of salt, an increase in temperature and other medium effects. At low salt concentrations, the DLVO theory predicts that the contribution of the van der Waals attraction is very small and the repulsive forces are dominant. At higher salt concentrations, however, the electrical double layer is so small that the inter-particle distance is reduced and the particles tend to aggregate irreversibly by van der Waals forces.

The citrate capping provides an electrostatic repulsion between the nanoparticles, but is only weakly bound to the GNP surface. This citrate layer can easily be displaced by other capping agents that interact more strongly with the gold surface. Traditional capping agents for colloidal GNPs are molecules such as polymers [46], surfactants [47], dendrimers [48] and even peptides [49]. In our approach, mercapto alkanes were used. The mercapto alkane functionalized GNPs showed an enhanced stability toward salt induced aggregation compared to the citrate GNPs (0.03 M NaCl) as presented in table 1.

3.3.2. Effect of PEO-units. Chemisorption of mercapto alkanes **5**–**8** onto the gold nanoparticles made the particles stable in solutions containing more than 0.50 mM NaCl (table 1). The inclusion of PEO-units resulted in the superior stabilization of these GNPs compared to mercapto alkane **4**. PEO-decorated GNPs are known to be stable even in highly electrolytic environments [50, 51]. These results are in agreement with Weisbecker *et al* [52], who reported that mercapto alkanes with at least three PEO-units do not easily flocculate in a wide range of ionic strengths and pH values. It is expected that this stabilization effect of PEO-mercapto alkanes is only slightly dependent on the surface charge as a small repulsive interaction may arise from negative charges due to a bound layer of hydroxide ions. However, steric or entropic effects of the PEO-layer will be more important to keep the particles dispersed [36]. The entropy is unfavorably decreased

as two hydrophilic surfaces approach each other due to the disruption of hydrogen bonds [53]. In other words, the PEO moieties of the GNPs attract water molecules more strongly than they attract each other, so that they repel one another as a net result [54]. As such steric or entropic effects will keep the PEO coated GNPs dispersed.

3.3.3. Collective effects of PEO-units and end-groups. By changing the end-group from OH (**5**) to COOH (**6**), the stability of the mercapto alkane functionalized GNPs increases clearly from 0.5 to 1 M NaCl. Furthermore, by increasing the amount of PEO-units (from 3 to 6) superior stabilization was obtained, up to 2 M NaCl. Based on the results presented in table 1, it can be concluded that both the end-group and the PEO-units determine the final stability of the mercapto alkane functionalized GNPs in an electrolytic environment. By comparing the zeta potential measurements, the surface charge is more negative when mercapto alkanes with a carboxylic end-group are used compared to a hydroxylic end-group, as stated earlier (see table 1). This implies that these GNPs are more stable towards salt induced aggregation. Remarkably, the surface charge of citrate and mercapto alkane **4** capped GNPs (respectively −42.5 and −48.6 mV) are lower compared to the zeta potential obtained for mercapto alkane (**5**, **7**) decorated GNPs (−22.3, −15.5 mV). Nevertheless, they are less stable in a high salt environment. This discrepancy can be explained by the fact that the GNP stability is not only affected by electrostatic stabilization, but steric or entropic effect will also influence the GNP stability, as stated earlier. Therefore, by including mercapto alkanes with a carboxylic end-group (**6**, **8**) instead of a hydroxylic one (**5**, **7**), the electrostatic stabilization of the GNPs was further improved. In the latter case, the electrostatic, steric or entropic effects were combined to reach extreme stabilization. In this way, GNPs were stabilized up to a concentration of 2 M NaCl by using mercapto alkane **8**. The corresponding UV–vis absorption spectra are shown in figure 2(b).

3.3.4. Effect of the mercapto alkane concentration. Reducing the mercapto alkane concentration in the synthesis protocol led to a less dense coverage of the GNPs and hence a lower stability of the GNPs. This was verified by UV–vis absorption spectroscopy. The plasmon band shifted to higher wavelength at increasing density of the capping layer. At a concentration of 1 mM mercapto alkanes, a saturation level was obtained for all investigated nanoparticles (data not shown). This concentration of mercapto alkanes is also sufficient to stabilize the GNPs under physiological conditions as shown in figure 3. The concentration of mercapto alkane **8** can be decreased to 0.10 mM, and still reach extreme stabilization in 2 M NaCl.

3.4. Characterization of DNA and mercapto alkane co-loaded GNPs

To functionalize the GNPs with DNA, the simultaneous adsorption of mercapto alkanes and ssDNA was examined. To this aim, mercapto alkane **8** was used, because of its stabilizing properties when immobilized onto the GNP surface, even at

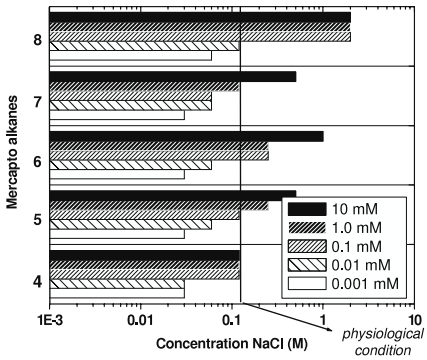

Figure 3. The mercapto alkane density onto the GNPs was changed by changing the initial concentration (10 mM) of mercapto alkanes (**4**–**8**) used in the synthesis protocol (0.001–10 mM). The maximum concentration of NaCl is presented, whereby the GNPs do not show a λ_{LSPR} shift and hence no aggregation.

low concentrations. In order to have free space for the ssDNA or to induce competition between the ssDNA and mercapto alkanes on the nanoparticle surface, the concentration of mercapto alkane **8** was further optimized. Both, UV–vis absorbance and DLS measurements revealed that the final concentration of mercapto alkane **8** needs to exceed 2.3 μM to sufficiently coat the GNP and to avoid aggregation in high electrolytic hybridization buffer (see figure 4). The simultaneous addition of 25-nct-11 (0.9 μM) and mercapto alkane **8** (2.3 μM) increased the hydrodynamic diameter by 2.5 nm compared to the GNPs without ssDNA (mercapto alkane **8**, 4.5 μM), suggesting a successful coupling of the 25-nct-11 onto the GNP surface. When higher concentrations of mercapto alkanes were used (4.5 μM) together with 25-nct-11 (0.9 μM), the hydrodynamic diameter increased, but somewhat less (2.1 nm). The simultaneous chemisorption of mercapto alkanes and 25-nct-11 has a more pronounced effect on the hydrodynamic diameter compared to the LSPR absorption wavelength. A non-significant wavelength shift was obtained when simultaneously thiolated ssDNA and mercapto alkanes were deposited on the GNP surface compared to solely mercapto alkanes. The absorbance of the ssDNA and mercapto alkane **8** coated GNPs, on the other hand, is higher than their corresponding GNPs coated solely with mercapto alkane **8**. This means that the particles are more stable and survive the washing steps more easily when the ssDNA is present. From the UV–vis absorbance and DLS measurements we can conclude that the co-loading with ssDNA and mercapto alkane **8** is successful, and their stability is preserved in hybridization buffer.

3.5. Hybridization efficiency of the DNA and mercapto alkane co-loaded GNPs and their potential towards DNA sensing

To determine whether the DNA and mercapto alkane **8** co-loaded GNPs could be used for DNA sensing, different sets of experiments were performed using SPR. First, the hybridization efficiency of the DNA functionalized GNPs (2.3 μM, **8** + 25-nct-11 and 4.5 μM, **8** + 25-nct-11) was studied and shown in figure 5(a) for both a complementary and a non-complementary immobilized DNA probe (respectively

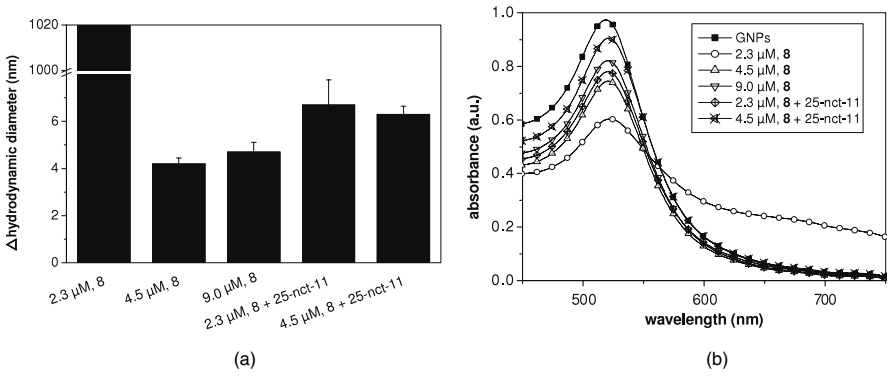

Figure 4. (a) The increase in hydrodynamic diameter for GNPs coated with different amounts of HS–$(CH_2)_{11}$–PEO_6–COOH (**8**) and 25-nct-11 stored in hybridization buffer. By the addition of solely 2.3 μm **8**, the nanoparticles aggregate. The precise hydrodynamic diameter could not be measured accurately because the aggregates were larger than 1 μm. (b) The corresponding UV–vis absorption spectra of the various GNPs in hybridization buffer. The values expressed in μM represent the final concentration of mercapto alkane **8** used in the synthesis procedure. As a reference, the citrate capped GNP in H_2O were plotted.

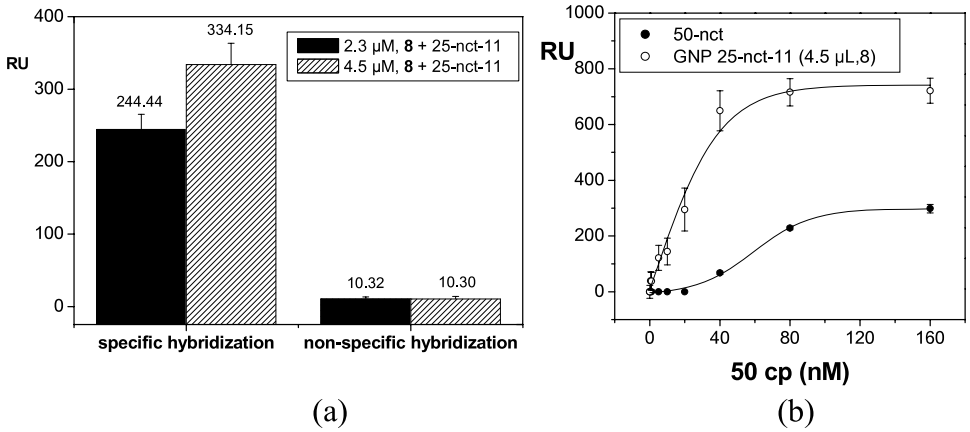

Figure 5. (a) The hybridization efficiencies, measured by SPR, of DNA (25-nct-11) and mercapto alkane (**8**) co-loaded GNPs. The concentration of mercapto alkane **8** was varied. (b) The detection of 50-nct by SPR for both, a direct detection method and a sandwich approach using DNA modified GNPs.

25-nct-c-6, 25-nct-6). The obtained hybridization of 25-nct-11 functionalized GNPs is very specific (>240 RU) towards binding of the immobilized 26-nct-c-6, while the non-specific binding observed is only 3.1–4.2%. Furthermore, the lowest percentage of non-specific hybridization was observed for the nanoparticles bearing the highest concentration of mercapto alkanes (4.5 μM, **8** + 25-nct-11). Apart from the fact that the latter are more stable, the higher percentage of PEO also contributes to a lower non-specific binding. One would expect that the nanoparticles bearing the lowest amount of mercapto alkanes, and thus relatively more immobilized thiolated DNA, would give rise to a more efficient hybridization. However, the experimental results proved the opposite as also recently reported [55]. GNPs bearing a higher concentration of mercapto alkanes, probably favor the upright orientation of the co-loaded thiolated DNA, resulting in a more specific hybridization [27].

Second, the GNPs bearing the highest concentration mercapto alkanes (4.5 μM, **8** + 25-nct-11) were used in a sandwich approach for the detection of ssDNA. In a first step, immobilized 25-nct-3 was hybridized with different concentrations 50-nct. Additionally, 25-nct-11 functionalized GNPs were hybridized which specifically bind the 50-nct in a sandwich structure. As shown in figure 5(b), the detection of 50-nct was improved tenfold by the hybridization with the GNPs (LOD 2.5 nM compared to 25 nM without GNPs [56]).This preliminary result can be further improved by optimizing the concentration of GNPs and the immobilization procedure of the 25-nct-3.

4. Conclusions

GNPs were coated with a variety of mercapto alkanes. The mercapto alkane stabilizing properties were extensively studied by comparing the hydrodynamic diameter, zeta potential and LSPR characteristics of the GNPs. The best stabilizing results were obtained by using mercapto alkanes with a sufficiently long alkane chain, PEO-units and a charged end-group. GNPs coated with a mercapto alkane fulfilling these requirements, e.g. $HS(CH_2)_{11}PEO_6COOH$, appeared to be stable in 2 M NaCl.

Furthermore, a one-step synthesis route was introduced for coating GNPs with ssDNA. The DNA functionalized GNPs were stable in a highly electrolytic environment and showed a

very specific hybridization with their complementary ssDNA immobilized on a planar gold substrate. Furthermore, these DNA functionalized GNPs allowed the sensitive detection of ssDNA in a sandwich approach. The DNA functionalized gold nanoparticles exhibit promising potential for use in advanced biosensor technologies where high salt environments are mandatory.

Acknowledgments

This work was partly supported by the 'Institute for the Promotion of Innovation through Science and Technology in Flanders' (IWT-Vlaanderen) and the European Commission (FP6, SmartHEALTH 016817). We thank the colleagues of IMEC for their assistance during the preparation of the manuscript. In addition, we thank Dr F Frederix for the synthesis and characterization of the $HS(CH_2)_6PEO_3OH$ and Dr A Van Aerschot for the synthesis of the oligonucleotide modified with the 5′-mercapto-11-undecyl hexa(ethylene oxide) linker [27].

References

[1] Liz-Marzán L M 2006 *Langmuir* **22** 32–41
[2] Moores A and Goettman F 2006 *New J. Chem.* **30** 1121–32
[3] Maier S and Atwater H A 2005 *J. Appl. Phys.* **98** 011101
[4] Stephan L and El-Sayed M A 1999 *J. Phys. Chem.* B **103** 4212–7
[5] Miller M M and Lazarides A A 2005 *J. Phys. Chem.* B **109** 21556–65
[6] Frederix F, Friedt J M, Choi K H, Laureyn W, Campitelli A, Mondelaers D, Maes G and Borghs G 2003 *Anal. Chem.* A **75** 6894–900
[7] Liu J W and Lu Y 2003 *J. Am. Chem. Soc.* **125** 6642–3
[8] Haes A J, Stuart D A, Nie S and Van Duyne R P 2004 *J. Fluorescence* **14** 355–67
[9] Elghanian R, Storhoff J J, Mucic R C, Letsinger R L and Merkin C A 1997 *Science* **277** 1078–81
[10] Javier D J, Nitin N, Levy M, Ellington A and Richards-Kortum R 2008 *Bioconju. Chem.* **19** 1309–12
[11] Giljohann D A, Seferos D S, Prigodich A E, Patel P C and Mirkin C A 2009 *J. Am. Chem. Soc.* **131** 2072–3
[12] Weiler J, Causepohl H, Hauser N, Jensen O N and Hoheisel J D 1997 *Nucl. Acid Res.* **25** 2792–9
[13] Porter M D, Bright T B, Allara D L and Chidsey C E 1987 *J. Am. Chem. Soc.* **109** 3559–68
[14] Srisombat L O, Park J S, Zhang S and Lee T R 2008 *Langmuir* **24** 7750–4
[15] Zolk A, Eisert F, Pipper J, Herrwerth S, Eck W, Buck M and Grunze M 2000 *Langmuir* **16** 5849–52
[16] Jans K, Bonroy K, De Palma R, Reekmans G, Jans H, Laureyn W, Smet M, Borghs G and Maes G 2008 *Langmuir* **24** 3949–54
[17] Hostetler M *et al* 1998 *Langmuir* **14** 17–30
[18] Lin S Y, Tsai Y T, Chen C C, Lin C M and Chen C H 2004 *J. Phys. Chem.* B **108** 2134–9
[19] Brust M, Walker M, Bethell D, Schiffrin D J and Whyman R 1994 *J. Chem. Soc., Chem. Commun.* 801–2
[20] Song Y and Murray R W 2002 *J. Am. Chem. Soc.* **124** 7096–102
[21] Templeton A C, Wuelfing W P and Murray R W 2000 *Acc. Chem. Res.* **33** 27–36
[22] Hostetler M J, Templeton A C and Murray R W 1999 *Langmuir* **15** 3782–9
[23] Patel N, Davies M C, Hartshorne M, Heaton R J, Roberts C J, Tendler S J B and Williams P M 1997 *Langmuir* **13** 6485–90
[24] Nie L B, Yang Y, Li S and He N Y 2007 *Nanotechnology* **18** 305501–5
[25] Hurst S J, Lytton-Jean A K R and Mirkin C A 2006 *Anal. Chem.* **78** 8313–8
[26] Mirkin C A, Letsinger R L, Mucic R C and Storhoff J J 1996 *Nature* **382** 607–9
[27] Van Aerschot A and Rozenski J 2006 *J. Am. Soc. Mass Spectrom.* **17** 1396–400
[28] Kimling J, Maier M, Okenve B, Kotaidis V, Ballot H and Plech A 2006 *J. Phys. Chem.* B **110** 15700–07
[29] Turkevich J, Stevenson P C and Hillier J 1951 *Discuss. Faraday Soc.* **11** 55–75
[30] Bellino M G, Calvo E J and Gordillo G 2004 *Phys. Chem. Chem. Phys.* **6** 424–8
[31] Liu X, Atwater M, Wang J and Huo Q 2007 *Colloids Surf.* **58** 3–7
[32] Patungwasa W and Hodak J H 2008 *Mater. Chem. Phys.* **108** 45–54
[33] Stakenborg T, Peeters S, Reekmans G, Laureyn W, Jans H and Imberechts H 2008 *J. Nanopart. Res.* **10** 143–52
[34] Peeters S, Stakenborg T, Reekmans G, Laureyn W, Lagae L, Van Aerschot A and Van Ranst M 2008 *Biosens. Bioelectron.* **24** 72–7
[35] Herne T M and Tarlov M J 1997 *J. Am. Chem. Soc.* **119** 8916–20
[36] Zhang F, Skoda M W A, Jacobs R M J, Zorn S, Martin R A, Martin C M, Clark G F, Goerigk G and Scheiber F 2007 *J. Phys. Chem.* A **111** 12229–37
[37] Dobrovolskaia M A, Patri A K, Zheng J, Clogston J D, Ayub N, Aggarwal P, Neun B W, Hall J B and McNeil S E 2009 *Nanomedicine* **5** 106–17
[38] Jans H, Liu X, Austin L, Maes G and Huo Q 2009 *Anal. Chem.* **81** 9425–32
[39] Malinsky M D, Kelly K L, Schatz G C and Duyne R P 2001 *J. Am. Chem. Soc.* **123** 1471–82
[40] Buecker P, Trileva E, Himmelhaus M and Dahint R 2008 *Langmuir* **24** 8229–39
[41] Imamuraa K, Shimomuraa M, Nagaia S, Akamatsua M and Nakanishi K 2008 *J. Biosci. Bioeng.* **106** 273–8
[42] Sylvestre J P, Kabashin A V, Sacher E, Meunier M and Luong J H T 2004 *J. Am. Chem. Soc.* **126** 7176–7
[43] Werner C, König U, Augsburg A, Arnhold C, Körber H, Zimmermann R and Jacobasch H J 1999 *Colloids Surf.* **159** 519–29
[44] Hermanson G T 2008 *Bioconjugate Techniques* 2nd edn, Pierce Biotechnology (Tockford: Thermo Fishier Scientific) chapter 24
[45] Browen W R and Sharif A O 1998 *Nature* **393** 663–6
[46] Mandal T K, Fleming M S and Walt D R 2002 *Nano Lett.* **2** 3–7
[47] Mortier T, Persoons A and Verbiest T 2006 *Cent. Eur. J. Chem.* **4** 160–5
[48] Crooks R M, Zhao M, Sun L, Chechik V and Yeung L Y 2001 *Acc. Chem. Res.* **34** 181–90
[49] Brewer S H, Glomm W R, Johnson M C, Knag M K and Franzen S 2005 *Langmuir* **21** 9303–7
[50] Kanaras A G, Kamounah F S, Schaumburg K, Kiely C J and Brust M 2002 *Chem. Commun.* 2294–5
[51] Zhang F, Dressen D G, Skoda M W A, Jacobs R M J, Zorn S, Martin R A, Marting C M, Clark G F and Schreiber F 2008 *Eur. Biophys. J.* **37** 551–61
[52] Weisbecker C S, Merritt M V and Whitesides G M 1996 *Langmuir* **12** 3763–72
[53] Preston T C, Nuruzzaman M, Jones N D and Mittler S 2009 *J. Phys. Chem.* C **113** 14236–44
[54] Jan van Oss C 2008 *The Properties of Water and Their Role in Colloidal and Biological Systems* (London: Elsevier/Academic) pp 119–20
[55] Zu Y and Gao Z 2009 *Anal. Chem.* **81** 8523–8
[56] De Palma R, Reekmans G, laureyn W, Borghs G and Maes G 2007 *Anal. Chem.* **79** 7540–8